Elastic properties of noncarbon nanotubes as compared to carbon nanotubes

Aleksey Kochaev*

Department of Physics, Ulyanovsk State Technical University, 32 Severny Venets Street, 432027, Russia

(Received 22 July 2017; revised manuscript received 12 September 2017; published 11 October 2017)

A comparative study of stability, structural, and elastic properties of single-wall noncarbon nanotubes, including BN, AlN, GaN, AlP, GaP, and B nanotubes using *ab initio* simulation is presented. The proposed nanotubes can be found in nature, which is confirmed by calculation of their binding energy. The values of Young's modulus and Poisson's ratio for (0,n) and (n,n) proposed nanotubes with $n = 3 \ldots 20$ are obtained. The conception of two-dimensional (2D) Young's modulus of planar and tubular materials was developed. The calculations show that stable forms of boron nitride nanotubes have the 2D Young's modulus almost similar to carbon nanotubes. At the same time, it is stated that boron nanotubes have a higher 2D Young's modulus than any other known carbon and noncarbon nanostructures.

DOI: 10.1103/PhysRevB.96.155428

I. INTRODUCTION

A small size [1–4], thermal stability [5–7], mechanical strength [8–12], high surface area [13,14], and controllability of electric properties [15–20] allow us to consider nanotubes very promising materials for a various scope of engineering and technology. In the second half of the 20th century, there appeared physical geometrical models and some experimental research on nanoscale structures, including spatial tubular nanostructures [21–23]. These data were not taken into account seriously until 1991.

It is generally accepted that nanotubes were first prepared from carbon by Iijima [24] at that time. Carbon nanotubes are hollow cylinders formed by a rolled graphite layer. The next year, the first noncarbon nanotubes based on molybdenum and tungsten disulfides were synthesized [25]. Later, it was shown that other chemical elements and compounds can also form similar tubes [26–30]. The further development of the notion of noncarbon nanotubes was made either by synthesis or simulations with subsequent prediction of their structures and properties [31–35]. At present, these approaches irrespective of each other result in "discovery" of nanotubes based on various chemical elements (and their compounds) of the 12th–15th groups of the periodic table [31] as well as some "exotic nanotubes" based on some chemical elements of the 16th group [36].

The elastic properties of noncarbon nanotubes were investigated for almost two decades [27,36] (carbon nanotubes even longer [37–39]). However, the congruence of elastic characteristics (e.g. Young's modulus) of carbon and noncarbon nanotubes obtained by different experimental and theoretical methods is worse than when their electronic properties (e.g. band gap) are investigated [31]. The lack of high accuracy is due to the following reasons:

(1) Synthesized nanotubes are not always similar to their geometrical models. These nanotubes often have an irregular shape, many inclusions, and defects. Thus, nanotubes obtained in different laboratories differ from each other, even if they are the same in chemical composition. Production of "pure" nanotubes remains a complex nanotechnical problem.

(2) There are two theoretical approaches to the calculation of elastic characteristics of nanotubes. The first method is related to using an interaction potential which is not easy to describe when a nanotube consists of different atoms. The second regards a tube as a continuous shell. In this case, it is necessary to take into account the so-called "monolayer thickness" or thickness of a nanotube wall. Various authors do not share the same assumptions about the magnitude of this parameter for carbon nanotubes [40–42].

(3) The methodology associated with the concept of bulk deformations applied to single-wall nanotubes is incorrect. Really, the significance of the cross-sectional area on which the deforming force acts is undefined for one-dimensional (1D) and two-dimensional (2D) nanostructures. For more details, see Refs. [43,44].

Despite the fact that high precision of the Young's modulus for carbon nanotubes is not achieved, it is known that this elastic modulus has a record magnitude among classical materials. In Refs. [45–48], the authors obtained values from 0.5 to 5.5 TPa. The excellent result is due to the "perfect" hexagonal crystalline lattice of carbon nanotubes and strong covalent bonds between carbon atoms. The noncarbon nanotubes described in Ref. [31] have a graphenelike crystal structure. These are boron nitride (BN), aluminum nitride (AlN), gallium nitride (GaN), aluminum phosphide (AlP), and gallium phosphide (GaP) nanotubes. The considered nanotubes are wide-bandgap semiconductors or dielectrics having great potential applications in nanoelectronics and nano-optoelectronics.

If a center of each hexagon contains one additional atom, a crystal lattice becomes triangular. Boron nanotubes consist of rolled-up pieces of a triangular lattice in the form of an armchair or a zigzag [49,50]. Such nanotubes together with boron convex clusters [51] and spherical clusters [52,53] form a special class of boron nanostructures fully described in Ref. [54]. Among the electron deficient elements of the 13th group, only boron ($2s^2 2p^1$) can form strong covalent bonds. In this connection, pure boron compounds have neither a purely covalent nor a purely metallic character [49]. However, all nanotubes composed of boron atoms, despite their size and form, are metallic [49,55]. On the contrary, BN nanotubes exhibit dielectric properties with energy gap from 5.5 to 6.0 eV [31].

*a.kochaev@gmail.com

 ©2017 American Physical Society

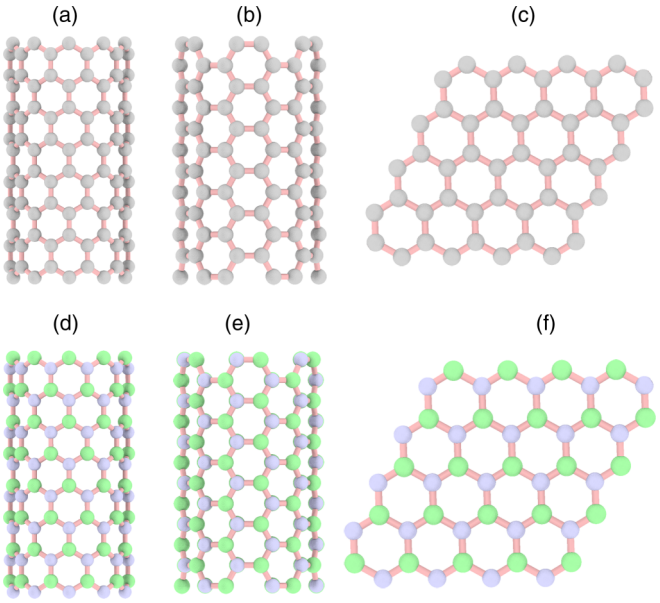

FIG. 1. The atomic models of the considered carbon and noncarbon ($A^{III}B^{V}$) nanotubes before optimization: (a) carbon nanotubes (0,5), (b) carbon nanotubes (10,10), (c) crystalline structure of graphene which can be rolled to nanotubes, (d) noncarbon nanotubes (0,5), (e) noncarbon nanotubes (10,10), and (f) crystalline structure of planar form $A^{III}B^{V}$ nanoallotropes. Here, gray balls indicate the carbon atoms, green balls indicate the A atoms, and light blue balls indicate the B atoms.

Since the mechanical characteristics of carbon nanotubes are unique, the elastic properties of *similar* noncarbon nanotubes can also cause an interest. The aim of this paper is to investigate the elastic characteristics of the thermodynamically stable single-wall nanotubes composed from boron atoms, boron compounds, and other atoms adjacent to a boron atom in the periodical table using *ab initio* simulation.

II. MATERIALS AND METHODS

The atomic models of the considered carbon and noncarbon ($A^{III}B^{V}$) nanotubes together with its planar form are shown in Fig. 1. The notation $A^{III}B^{V}$ means that symbol A can be atoms of B, Al, or Ga and symbol B is N or P.

The nanotubes presented in Fig. 1 have a hexagonal crystalline lattice type. Nanotubes with a hexagonal lattice type can be designated as h-C, h-BN, h-AlN, h-GaN, h-AlP, and h-GaP.

The remaining atomic models of considered noncarbon (from boron) nanotubes together with its planar form are shown in Fig. 2.

Nanotubes presented in Fig. 2 have a triangular crystalline lattice type. Nanotubes with a triangular lattice type can be designated as tri-B. The edges of boron nanotubes, like carbon nanotubes, are also of two types: zigzag and armchair (quasiarmchair).

The lattice parameters of all planar nanoallotropes [Figs. 1(c), 1(f), and 2(c)] were used to generate the coordinates of the atoms on a cylinder surface, and the sheet was wrapped to form the tubular structure [Figs. 1(a), 1(b), 1(d), 1(e), 2(a),

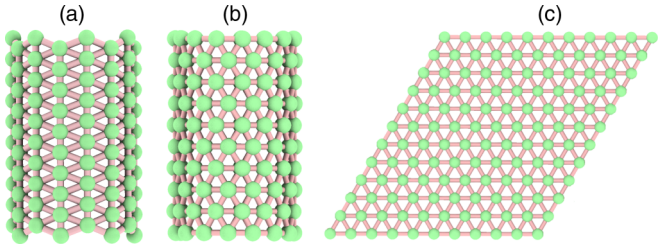

FIG. 2. The atomic models of the considered noncarbon (from boron) nanotubes before optimization: (a) boron nanotube (zigzag setting), (b) boron nanotube (armchair setting), and (c) crystalline structure of borophene, which can be rolled to nanotubes in the form of armchair or zigzag. Here, green balls indicate the boron atoms.

and 2(b)]. After using a structural optimization procedure for condensed systems, it is possible to obtain the equilibrium geometry for all nanotubes. The optimized atomic coordinates were used as the input data for the *ab initio* calculation to define the binding energy and strain energy. In Ref. [56], it is noted that, to determine the elastic constants, it is necessary to strain a crystalline structure and calculate the total energy response to the strain.

The corresponding calculations were performed by means of the density functional theory (DFT) implemented within the VASP 4.6 [57–59]. In all cases, ion cores were treated using Vanderbilt pseudopotentials [60]. Electron exchange and correlation effects were described by means of the corrected spin-polarized generalized gradient Perdew-Burke-Ernzerhof approximation [61]. The electronic wave function was expanded in a plane-wave basis set with an energy cutoff of 400 eV. Brillouin zone sampling was carried out using a Monkhorst-Pack mesh [62] of $1 \times 1 \times 37$ for all the cases. All calculations were carried out using periodic boundary conditions. To avoid the interaction between adjacent atoms in the direction perpendicular to the sheet, a lattice cell parameter much greater than a possible bond length was used (6 Å).

The binding energy per one atom E_b was calculated as follows [36]:

$$E_b = \frac{E_t - NE}{N}. \tag{1}$$

Here, E is the total energy of an isolated atom, N is the number of atoms in the translating cluster (unit cell), and E_t is the total energy of the cluster. The assumption was made that zero level of energy corresponds to disintegration of the system, i.e. $E < 0, E_t < 0$. Because $|E_t| > |NE|$, the binding energy turns out negative. This approach, which is in good agreement with the available theoretical and experimental results, is usually used to define the energetic stability [63–65].

As shown in Ref. [66], there are two main ways of extracting elastic data through *ab initio* simulation using the total energy of the strained materials and stress-strain relationship. The Young's modulus Y is calculated as the second derivative of the total energy E_t with respect to the strain along the longitudinal direction of a nanotube at the equilibrium parameters [67]

$$Y = \frac{1}{V_0}\left(\frac{\partial^2 E_t}{\partial \varepsilon^2}\right)_{\varepsilon=0}. \tag{2}$$

Here, V_0 is the equilibrium volume, ε is the relative extension. On the basis of a continuous shell model, the equilibrium volume for a single-wall carbon (or noncarbon) nanotubes can be defined as

$$V_0 = \pi L D \delta R, \tag{3}$$

where L and D denote the length and diameter of a nanotube, respectively; δR is the abovementioned "monolayer thickness"; here, it is the thickness of a tube wall [42].

For carbon nanotubes, the wall thickness is not well defined: in Ref. [45], the value $\delta R = 0.66$ Å is obtained by using the rolling energy formula of the graphite sheet vs $\delta R = 3.4$ Å [24] taken as an interwall distance of graphite. Furthermore, it is still unclear what value should be taken for the thickness of noncarbon nanotubes.

In Ref. [36], an alternative definition for Young's modulus was used, namely

$$Y_{2D} = \frac{1}{a_{1i}a_{1j}a_{1l}a_{1m}s_{ijlm}}. \tag{4}$$

Here, s_{ijlm} are the components of a tensor of elastic compliances in the crystallographic coordinate system, (a_{1n}) is the matrix of the directing cosines of a moving reference system in respect to the crystallographic axes [44]. The matrix representation of a fourth-rank tensor s_{ijlm} was used, i.e. a pair of symmetric indices is replaced by: $11 \rightarrow 1$; $22 \rightarrow 2$; $12,21 \rightarrow 3$. Such a representation is used for an elastic stiffness tensor c_{ijlm}.

The components of the elastic stiffness tensor were defined as $c_{ijlm} = \frac{\partial^2 F}{\partial \varepsilon_{ij} \partial \varepsilon_{lm}}$, where F is the potential strain energy (per unit of an area) of an elastic-deformed body, ε_{ij},ε_{lm} are the components of a strain tensor. The strain energy is the difference between the energies of stretched (or compressed) and relaxed nanotubes.

The relation between the elastic compliances s_{ij} and elastic stiffness c_{ij} is given by Ref. [68]

$$s_{ij} = \frac{(-1)^{i+j}\Delta c_{ij}}{\Delta^c}, \tag{5}$$

where Δ^c is the matrix determinant composed of elastic stiffness coefficients, and Δc_{ij} is a minor obtained from the determinant by crossing out the ith row and the jth column.

The relationships between s_{ij} and c_{ij} for the structures having a hexagonal lattice are given by Ref. [68]

$$s_{11} = \frac{c_{11}}{c_{11}^2 - c_{12}^2}, \quad s_{12} = -\frac{c_{12}}{c_{11}^2 - c_{12}^2}, \tag{6}$$

and for structures having a triangular lattice the relationships are as follows:

$$s_{11} = \frac{c_{22}}{c_{11}c_{22} - c_{12}^2}, \quad s_{12} = -\frac{c_{12}}{c_{11}c_{22} - c_{12}^2},$$
$$s_{22} = \frac{c_{11}}{c_{11}c_{22} - c_{12}^2}. \tag{7}$$

Using Eqs. (4) and (6), the relationship for the Young's modulus of the h-C, h-BN, h-AlN, h-GaN, h-AlP, and h-GaP nanotubes along their longitudinal direction is given by

$$Y_{2D} = \frac{c_{11}^2 - c_{12}^2}{c_{11}}. \tag{8}$$

Using Eqs. (4) and (7), the relationship for the Young's modulus of triangular nanotubes (along their longitudinal direction) is given by

$$Y_{2D} = \frac{c_{11}c_{22} - c_{12}^2}{c_{11}}. \tag{9}$$

Defined in this way, the elastic characteristic Y_{2D} "shows" an extremely 2D nature. Therefore, Y_{2D} [from Eq. (4)] is a 2D Young's modulus, which allows us to avoid the choice of the wall thickness [44,69,70].

The Poisson's ratio as a measure of the lateral compression along h accompanied by the tension along k [36,44] is given by Ref. [36]

$$\sigma = \frac{s_{hk}}{s_{kk}}, \tag{10}$$

where s_{hk} and s_{kk} are components of the elastic compliances also derived from the elastic moduli tensor using Eqs. (6) and (7).

In this paper, the linear elastic response regime is applied. The ratio $D/L < 0.1$ which corresponds to the case of long nanotubes was used everywhere.

III. RESULTS AND CONCLUSIONS

Flat and buckled boron nanotubes [49] having similar values of bond lengths and binding energy per atom are detected after all steps of optimization. The terms "flat" and "buckled" explain how the atoms are located on the surface of boron nanotubes. All boron atoms on the surface of flat nanotubes are at the same distance from its longitudinal axis. Contrary to flat boron nanotubes, the surface of buckled boron nanotubes is puckered [49].

The equilibrium values of bond lengths for all types of selected noncarbon nanotubes as compared to carbon nanotubes are given in Table I. It is well known that the bond length of nanotubes composed of the same atoms and having the same crystalline structure is almost independent of its diameter [71]. Therefore, the average values of bond lengths are listed in Table I.

We see that the bond lengths calculated in this paper are in the range of 1.42–2.40 Å and close to values given in other papers.

The equilibrium values of binding energy for all types of selected nanotubes as compared to carbon nanotubes are shown in Fig. 3.

One can see that the binding energy for all noncarbon nanotubes does not exceed (on modulus) 7.45 eV. It is slightly less than the binding energy of carbon nanotubes. Therefore, the thermodynamic stability of noncarbon nanotubes is worse too.

Figure 4 shows the 2D Young's modulus for selected $(0,n)$ nanotubes as compared to carbon nanotubes.

Figure 5 shows the 2D Young's modulus for all types of selected (n,n) nanotubes as compared to carbon nanotubes.

TABLE I. The average values of bond lengths (Å) for different types of carbon and noncarbon nanotubes after optimization.

	C	BN	AlN	GaN	AlP	GaP	B
This paper	1.42	1.47	1.77	1.84	2.40	2.20	1.68
Other	1.42 [71]	1.51 [72]	1.79 [73] 1.95 [74]	1.84 [75]	2.34 [76]	2.29 [77]	1.64 [50] 1.69 [49]

From Figs. 4(a) and 5(a), one can see that the 2D Young's modulus of selected ($A^{III}B^{IV}$) noncarbon nanotubes has lower elastic characteristics than carbon nanotubes. However, as it is shown in Figs. 4(b) and 5(b), the elastic characteristics of boron nanotubes are absolutely unique. If one takes into account the concept of three-center bonding, such a result seems likely. A detailed model of the three-center bonding is described in Ref. [50]. In addition, the result seems even more attractive due to the fact that individual samples of borophene have been already synthesized [78].

The 2D Young's modulus of the zigzag boron nanotubes (flat triangular) is almost equal to 1800 N/m. For buckled zigzag structure, it is slightly less. The 2D Young's modulus of armchair boron nanotubes (flat and buckled triangular) is about two times less than for the zigzag boron nanotubes. As it was rightly noted in Ref. [49], the anisotropy of the elastic properties for borophene sheets leads to a similar result. In the zigzag boron nanotubes, strong σ bonds lie along straight lines forming parallel chains. Stretching (or compressing) the zigzag boron nanotubes along its longitudinal direction will be much harder than stretching armchair nanotubes in the same direction.

Presented in Figs. 4(a), 4(b), 5(a), and 5(b), results are discussed in more details. The obtained dependence of the Young's modulus on the diameter is more complicated than it was previously known. Let us remember that, according to some papers, the Young's modulus increases with an increase in diameter [27]; in other papers, the opposite assumption

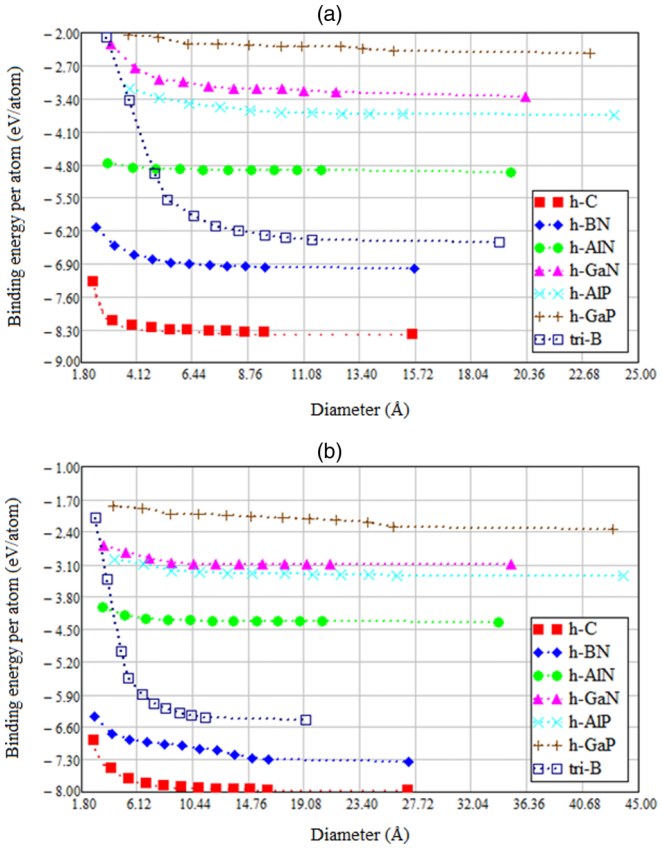

FIG. 3. The binding energy per atom as a function of the diameter for: (a) considered (0,n) nanotubes, and (b) considered (n,n) nanotubes. Each icon corresponds to the notation of chirality. For (0,n) nanotubes, it begins counting from $n = 3$ to 12 successively; the last icon (far right) corresponds to $n = 20$. For (n,n) nanotubes, it begins counting from $n = 2$ to 12 successively; the last icon (far right) corresponds to $n = 20$.

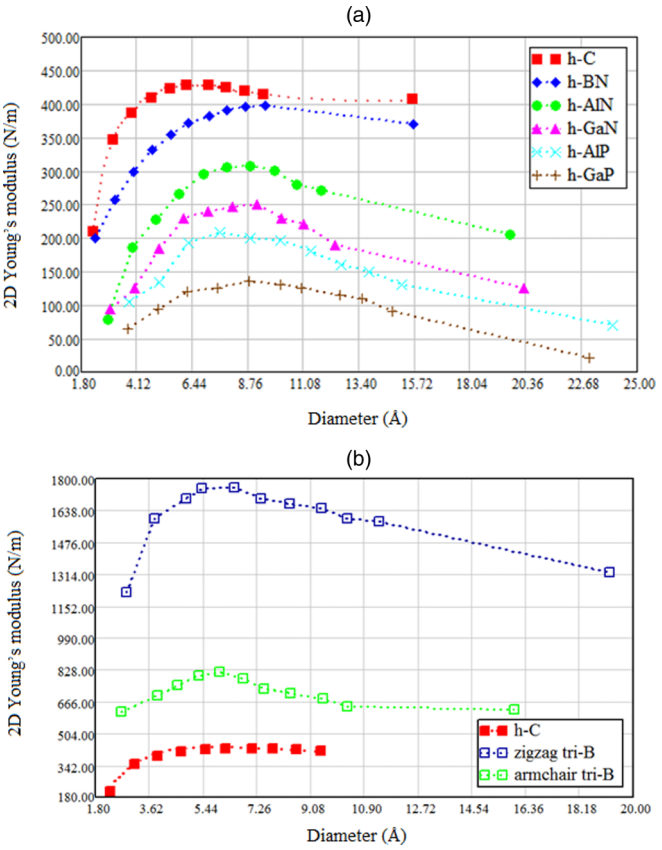

FIG. 4. 2D Young's modulus for: (a) $A^{III}B^{V}$ nanotubes (0,n) as compared to carbon nanotubes, and (b) buckled boron nanotubes as compared to carbon nanotubes. Each icon corresponds to the notation of chirality. For selected nanotubes, it begins counting from $n = 3$ to 12 successively; the last icon (far right) corresponds to $n = 20$.

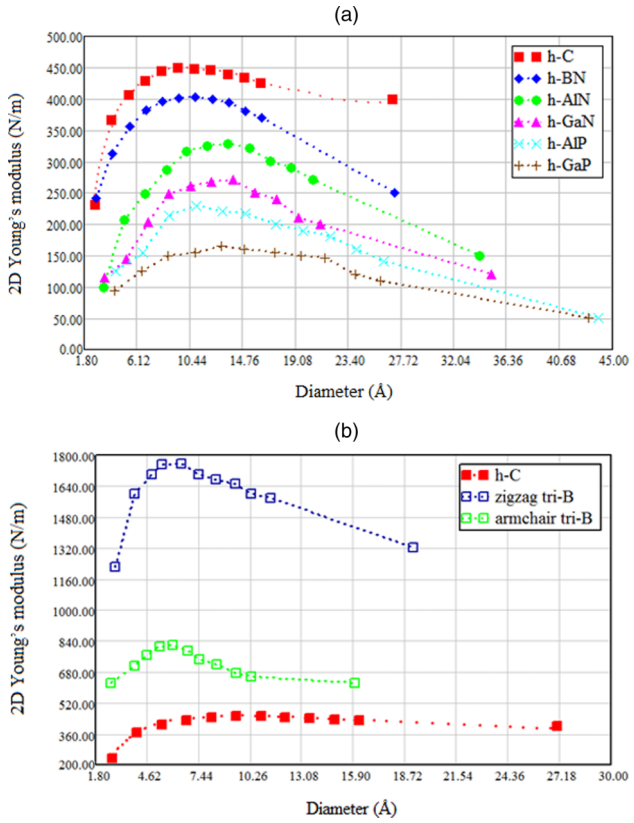

FIG. 5. 2D Young's modulus for: (a) $A^{III}B^{V}$ nanotubes (n,n) as compared to carbon nanotubes, and (b) flat boron nanotubes as compared to carbon nanotubes. Each icon corresponds to the notation of chirality. For selected nanotubes, it begins counting from $n = 2$ to 12 successively; the last icon (far right) corresponds to $n = 20$.

is made [48]; in the third type of paper, authors prove that the elastic properties of nanotubes are independent of their diameters and chiralities [38]. In our case, satisfying the condition $D/L < 0.1$, the 2D Young's modulus initially increases, reaching a maximum value, and then gradually decreases. We believe that such dependence is explained as follows: thin nanotubes have a small transverse size ($D < 5$ Å for boron nanotubes), so atoms on the "strongly rounded" walls interact with each other, reducing their overall rigidity. The binding energy per atom of such thin nanotubes is also low. When this interaction ceases, then the 2D Young's modulus is maximized ($D \approx 7$ Å for boron nanotubes). As the diameter of a nanotube increases ($D > 8$ Å for boron nanotubes), the curvature factor weakens, and the Young's modulus decreases to a value corresponding to the plane structure. In addition, using the *ab initio* simulation method, the preliminary geometry optimization is performed. As shown in Table I, the equilibrium geometry parameters (the bond lengths) obtained in this paper and recently published papers are quite similar. Unfortunately, we do not know if optimization in Refs. [27,38,48] was performed.

In Table II, the comparative elastic characteristics of tubular and planar structures are presented.

Using Table II, the values of Young's modulus introduced by different approaches can be compared. The values Y_{2D} and Y_{3D} (the bulk Young's modulus) of tubular and planar carbon and noncarbon nanotubes are given in the second and third columns, respectively. The bulk Young's modulus defined as $Y_{3D} = Y_{2D}/\delta R$ is given for additional comparison. In Refs. [27,69], for h-BN, authors assumed the value $\delta R = 3.4$ Å, which is not very reliable, of course. Therefore, it can only be used as a rough estimate of the bulk Young's modulus in this paper.

TABLE II. Comparative table of the elastic characteristics of some carbon and noncarbon structures.

			Y [from Eq. (2)] (N/m) depending on choice of the δR		
	Y_{2D} (N/m)	Y_{3D} (TPa)	0.66 Å [45]	1.3 Å [79]	3.4 Å [69]
h-C (10,10)					
This paper	436	1.28			467
Other papers		0.5÷5.0 [45–48]	350 [45]		423 [69]
Graphene					
This paper	353	1.04			381
Other papers	327 [44]	0.9÷2.8 [81,82]		365 [79]	
	342 [80]				
h-BN (10,10)					
This paper	387	1.14			354
Other papers		0.90 [27]			306 [69]
BN sheet					
This paper	264	0.78			291
Other papers	275 [80]				
	279 [83]				
Buckled tri-B (0,5)					
This paper	1680				
Buckled tri-B (5,5)					
This paper	825				
Borophene (Y in perpendicular directions)					
This paper	998; 637				
Other papers		0.87; 0.42 [49]			

TABLE III. Poisson's ratio for carbon and noncarbon nanotubes (0,10) and (10,10).

	C	BN	AlN	GaN	AlP	GaP
(0,10)	0.58	0.57	0.55	0.55	0.51	0.52
(10,10)	0.57	0.56	0.52	0.53	0.51	0.51

The values Y [from Eq. (2)] depending on the choice of δR are also presented. As shown in Table II, a strong dependence of the Young's modulus Y on the parameter δR is observed.

The values of Poisson's ratio for noncarbon nanotubes (0,10) and (10,10) as compared to carbon nanotubes are given in Table III.

For boron nanotubes, the Poisson's ratio calculated in this paper is 0.60, and it almost does not depend on the diameter. The article in Ref. [84] shows that Poisson's ratio for the planar 2D supracrystal and wide carbon nanotubes is 0.62.

To summarize, a detailed study of the energetic, structural, and elastic properties of certain noncarbon nanotubes has been carried out. In present calculations, the mutual influence of atoms on adjacent sides of nanotubes was taken into account, which also allows us to investigate the corresponding properties of thin nanotubes properly. The calculation demonstrated that the GaP, GaN, and AlP nanotubes are energetically metastable structures. The binding energy of the remaining nanotubes indicates rather good thermal stability (less than for carbon nanotubes), and it is commensurable with the binding energy of some fullerenes [85].

On the basis of the continuum theory of elasticity, the elastic characteristics for rather long nanotubes were obtained. The chirality indices for each type of noncarbon hexagonal nanotube corresponding to the maximum values of Young's modulus were obtained, which makes it possible to use the stiffest ones in practical applications. The agreement between the present results and the data from other theoretical and experimental works for carbon and noncarbon nanotubes was shown. The results indicate that h-BN nanotubes are close to carbon nanotubes as far as their elastic properties are concerned. Combining this feature with their wide-bandgap character makes them suitable for applications where electrically insulating high-strength materials are needed. Since the 2D nanoallotrope of boron—borophene—has been synthesized recently, an interest in its compounds appeared again. The excellent stiffness of boron nanotubes will certainly be used in many aspects of nanotechnology.

ACKNOWLEDGMENTS

This paper was funded by Russian Foundation for Basic Research, according to Research Project No. 16-32-60041 mol_a_dk. Also, I acknowledge a useful discussion with Dr. Rudolf Brazhe from Ulyanovsk State Technical University (Ulyanovsk, Russia).

[1] M. Scarselli, P. Castrucci, and M. De Crescenzi, J. Phys.: Cond. Matt. **24**, 313202 (2012).
[2] A. Maiti, C. J. Brabec, C. Roland, and J. Bernholc, Phys. Rev. B **52**, 14850 (1995).
[3] M. A. Grado-Caffaro and M. Grado-Caffaro, Optic **116**, 459 (2005).
[4] A. Tounsi, H. Heireche, H. M. Berrabah, A. Benzair, and L. Boumia, J. Appl. Phys. **104**, 104301 (2008).
[5] X. Wei, M. S. Wang, Y. Bando, and D. Golberg, Sc. Tech. Adv. Mat. **12**, 044605 (2011).
[6] K. M. Liew, C. H. Wong, X. Q. He, and M. J. Tan, Phys. Rev. B **71**, 075424 (2005).
[7] A. Mahajan, A. Kingon, Á. Kukovecz, Z. Konyac, and P. Vilarinho, Mat. Lett. **90**, 165 (2013).
[8] M. F. Yu, O. Lourie, M. J. Dyer, K. Moloni, T. F. Kelly, and R. S. Ruoff, Science **287**, 637 (2000).
[9] Y. H. Yang and W. Z. Li, Apll. Phys. Lett. **98**, 041901 (2011).
[10] M. Minary-Jolandan and M. F. Yu, J. Appl. Phys. **103**, 073516 (2008).
[11] S. Yu. Davydov and O. V. Posrednik, Phys. Sol. St. **57**, 837 (2015).
[12] H. J. Qi, K. B. K. Teo, K. K. S. Lau, M. C. Boyce, W. L. Milne, J. Robertson, and K. K. Gleason, J. Mech. Phys. Sol. **51**, 2213 (2003).
[13] J. J. Niu, J. N. Wang, Y. Jiang, L. F. Su, and M. Jie, Micropor. Mesopor. Mat. **100**, 1 (2007).
[14] M. A. Worsley, J. D. Kuntz, P. J. Pauzauskie, O. Cervantes, J. M. Zaug, A. E. Gash, J. H. Satcher, Jr., and Th. F. Baumann, J. Mater. Chem. **19**, 5503 (2009).
[15] J. González, Phys. Rev. B **67**, 014528 (2003).
[16] S. Rochel, J. Jiang, L. E. F. Torres, and R. Saito, J. Phys: Cond. Matt. **19**, 183203 (2007).
[17] D.-m. Sun, M. Y. Timmermans, T. Ying, A. G. Nasibulin, E. I. Kauppinen, S. Kishimoto, T. Mizutani, and Y. Ohno, Nat. Nanotech. **6**, 156 (2011).
[18] P. R. Bandaru, J. Nanosci. Nanotechnol. **7**, 1239 (2007).
[19] M. Miao, Carbon **49**, 3755 (2011).
[20] R. A. Brazhe and R. M. Meftakhutdinov, Tech. Phys. **61**, 750 (2016).
[21] D. E. H. Jones, New Scientist **31**, 493 (1966).
[22] A. Oberlin, M. Endo, and T. Koyama, Carbon **14**, 133 (1976).
[23] D. E. H. Jones, New Scientist **110**, 80 (1986).
[24] S. Iijima, Nature **354**, 56 (1991).
[25] R. Tenne, L. Margulis, M. Genut, and G. Hodes, Nature **360**, 444 (1992).
[26] X. Blase, A. Rubio, S. G. Louie, and M. L. Cohen, Europhys. Lett. **28**, 335 (1994).
[27] E. Hernandez, C. Goze, P. Bernier, and A. Rubio, Phys. Rev. Let. **80**, 4502 (1998).
[28] R. J. Baierle, S. B. Fagan, R. Mota, A. J. R. da Silva, and A. Fazzio, Phys. Rev. B **64**, 085413 (2001).
[29] G. Seifert and E. Hernandez, Chem. Phys. Let. **318**, 355 (2000).
[30] C. G. Rocha, A. Wall, A. R. Rocha, and M. S. Ferreira, J. Phys: Cond. Matt. **19**, 346201 (2007).
[31] A. L. Ivanovskii, Rus. Chem. Rev. **71**, 175 (2002).
[32] H. Guo, N. Lu, J. Dai, X. Wu, and X. C. Zeng, J. Phys. Chem. C **118**, 14051 (2014).

[33] M.-H. Park, Y. Cho, K. Kim, J. Kim, M. Liu, and J. Cho, Angew. Chem. Int. Ed. **50**, 9647 (2011).
[34] D. R. Cummins, H. B. Russell, J. B. Jasinski, M. Menon, and M. K. Sunkara, Nano Lett. **13**, 2423 (2013).
[35] J. F. C. Silva, J. D. Dos Santos, C. A. Taft, J. B. L. Martins, and E. Longo, J. Mol. Model. **23**, 204 (2017).
[36] A. I. Kochaev, AIP Advances **7**, 025202 (2017).
[37] R. S. Ruoff and D. C. Lorents, Carbon **33**, 925 (1995).
[38] J. P. Lu, Phys. Rev. Lett. **79**, 1297 (1997).
[39] E. W. Wong, P. E. Sheehan, and C. M. Lieber, Science **277**, 1971 (1997).
[40] Y. Huang, J. Wu, and K. C. Hwang, Phys. Rev. B **74**, 245413 (2006).
[41] F. Scarpa and S. Adhikari, J. Phys. D: Appl. Phys. **41**, 085306 (2008).
[42] S. Y. Kim and H. S. Park, J. Appl. Phys. **110**, 054324 (2011).
[43] O. E. Glukhova and O. A. Terent'ev, Phys. Sol. St. **48**, 1411 (2006).
[44] R. A. Brazhe, V. S. Nefedov, and A. I. Kochaev, Phys. Sol. St. **54**, 1430 (2012).
[45] B. I. Yakobson, C. J. Brabec, and J. Bernholc, Phys. Rev. Lett. **76**, 2511 (1996).
[46] C. F. Cornwell and L. T. Wille, Sol. St. Comm. **101**, 555 (1997).
[47] T. Halicioglu, Thin Sol. Films **312**, 11 (1998).
[48] Z. Xin, Z. Jianjun, and O.-Y. Zhong-can, Phys. Rev. B **62**, 13692 (2000).
[49] J. Kunstmann and A. Quandt, Phys. Rev. B **74**, 035413 (2006).
[50] H. Tang and S. Ismail-Beigi, Phys. Rev. Let. **99**, 115501 (2007).
[51] I. Boustani, Int. J. Quant. Chem. **52**, 1081 (1994).
[52] I. Boustani, Phys. Rev. B **55**, 16426 (1997).
[53] I. Boustani and A. Quandt, Eurphys. Lett. **39**, 527 (1997).
[54] I. Boustani and A. Quandt, ChemPhysChem **6**, 2001 (2005)
[55] A. Ricca and C. W. Bauschlicher, Chem. Phys. **208**, 233 (1996).
[56] P. Söderlind, O. Eriksson, J. M. Wills, and A. M. Boring, Phys. Rev. B **48**, 5844 (1993).
[57] G. Kresse and J. Furthmüller, Phys. Rev. B **54**, 11169 (1996).
[58] G. Kresse and J. Furthmüller, Comput. Mat. Sci. **6**, 15 (1996).
[59] G. Kresse and J. Furthmüller, *VASP the Guide* (University of Vienna, 2009), http://cms.mpi.univie.ac.at/vasp/.
[60] D. Vanderbilt, Phys. Rev. B **41**, 7892 (1990).
[61] J. P. Perdew, K. Burke, and M. Ernzerhof, Phys. Rev. Lett. **77**, 3865 (1996).
[62] H. T. Monkhorst and J. D. Pack, Phys. Rev. B **13**, 5188 (1976).
[63] P. Koskinen, S. Malola, and H. Hakkinen, Phys. Rev. Lett. **101**, 115502 (2008).
[64] B. I. Dunlapy and J. C. Boetger, J. Phys. B: At. Mol. Opt. Phys. **29**, 4907 (1996).
[65] V. V. Ivanovskaya, A. Zobelli, D. Teillet-Billy, N. Rougeau, V. Sidis, and P. R. Briddon, Eur. Phys. J. B **76**, 481 (2010).
[66] Y. Le Page and P. Saxe, Phys. Rev. B **65**, 104104 (2002).
[67] Y.-R. Jeng, P.-C. Tsai, and T.-H. Fang, Nanotech. **15**, 1737 (2004).
[68] J. F. Nye, *Physical Properties of Crystals* (Clarendon, Oxford, 1985)
[69] C. Goze, L. Vaccarini, L. Henrard, P. Bernier, E. Hernandez, and A. Rubio, Synth. Met. **103**, 2500 (1999).
[70] R. A. Brazhe and A. I. Kochaev, Phys. Sol. St. **54**, 1612 (2012).
[71] M. F. Budyka, T. S. Zyubina, T. G. Ryabenko, S. H. Lin, and A. M. Mebel, Chem. Phys. Lett. **407**, 266 (2005).
[72] M. Menon and D. Srivastava, Chem. Phys. Lett. **307**, 407 (1999).
[73] Z. Zhou, J. Zhao, Y. Chen, P. von Ragué Schleyer, and Z. Chen, Nanotech. **18**, 424023 (2007).
[74] S. M. Lee, Y. H. Lee, Y. G. Hwang, J. Elsner, D. Porezag, and T. Frauenheim, Phys. Rev. B **60**, 7788 (1999).
[75] D. C. Camacho-Mojica and F. López-Urías, Sci. Rep. **5**, 17902 (2015).
[76] S. V. Lisenkov, G. A. Vinogradov, and N. G. Lebedev, JETP Lett. **81**, 185 (2005).
[77] Mar. Mirzaei and Manh. Mirzaei, Monatsh. Chem. **142**, 111 (2011).
[78] A. J. Mannix, X.-F. Zhou, Br. Kiraly, J. D. Wood, D. Alducin, B. D. Myers, X. Liu, Br. L. Fisher, U. Santiago, J. R. Guest, M. J. Yacaman, A. Ponce, A. R. Oganov, M. C. Hersam, and N. P. Guisinger, Science **350**, 1513 (2015).
[79] J.-X. Shi, T. Natsuki, X.-W. Lei, and Q.-Q. Ni, Appl. Phys. Lett. **104**, 223101 (2014).
[80] R. C. Andrew, R. E. Mapasha, A. M. Ukpong, and N. Chetty, Phys. Rev. B **85**, 125428 (2012).
[81] J.-W. Jiang, J.-S. Wang, and B. Li, Phys. Rev. B **80**, 113405 (2009).
[82] J.-U. Lee, D. Yoon, and H. Cheong, Nano Lett. **12**, 4444 (2012).
[83] Q. Peng, W. Ji, and S. De, Comp. Mat. Sci. **56**, 11 (2012).
[84] R. A. Brazhe, A. A. Karenin, A. I. Kochaev, and R. M. Meftakhutdinov, Phys. Sol. St. **53**, 1481 (2011).
[85] K. S. Grishakov, K. P. Katin, and M. M. Maslov, Adv. Phys. Chem. 1862959 (2016).